

PACS numbers: 32.70.Jz; 42.62.Fi
DOI: 10.1070/QE2001v031n04ABEH001955

Temperature dependence of the collision broadening of the $^2P_{1/2} - {}^2P_{3/2}$ line of atomic iodine

M V Zagidullin, V D Nikolaev, M I Svistun, N A Khvatov

***Abstract*. The temperature dependence of the collision broadening of the spectrum of the $^2P_{1/2} \rightarrow {}^2P_{3/2}$ line of atomic iodine is determined in the 220 – 347 K range by the technique of high-resolution diode laser spectroscopy. The collision width in an oxygen–nitrogen medium depends on temperature as $(300\,\mathrm{K}/T)^{\gamma}$, where $\gamma = 0.87 \pm 0.13$.**

Keywords: *collision broadening, iodine atom, laser spectroscopy*.

1. Introduction

In connection with the development of an iodine photodissociation laser, the investigation of the collision broadening of the spectrum of the $^2P_{1/2} \rightarrow {}^2P_{3/2}$ transition in atomic iodine has attracted considerable attention [1 – 5]. Measurements of the broadening coefficients for this transition in different media were conducted at room temperature and above. In Ref. [4], an inversely proportional temperature dependence of the collision broadening gave the best fit to the measurements in the 300 – 1000 K range. In supersonic chemical oxygen – iodine lasers (OILs) at a pressure of the active medium of about 10 Torr and a temperature below 200 K, the contributions of collision and Doppler broadening mechanisms become comparable.

The technique of high-resolution diode laser spectroscopy has considerably improved the accuracy of scanning the $^2P_{1/2} \rightarrow {}^2P_{3/2}$ spectral line of atomic iodine [6, 7]. This method was used in Ref. [7] to scan the line of atomic iodine with a resolution of 6 MHz and to measure the coefficients of the collision broadening of the $^2P_{1/2} - {}^2P_{3/2}$ atomic iodine transition induced by nitrogen, helium, and oxygen at a temperature of 300 K.

The amplification (absorption) spectrum $g(X)$ of the strongest $^2P_{1/2}(F = 3) \rightarrow {}^2P_{3/2}(F = 4)$ atomic iodine transition is described in the case of a combined action of the Doppler and collision broadening mechanisms by the Voigt function, which is the convolution of a Gaussian function G with the full width at half maximum (FWHM) W_{D} and a Lorentz function L with the FWHM W_{L}:

$$g(X) = \Delta N \frac{A_{34}\lambda^2}{8\pi} L(X) * G(X) = \Delta N \frac{A_{34}\lambda^2}{8\pi} \Phi(X) = \Delta N \frac{A_{34}\lambda^2}{8\pi} \left(\frac{\ln 2}{\pi}\right)^{1/2} \frac{W_{\mathrm{L}}}{\pi W_{\mathrm{D}}} \int_{-\infty}^{\infty} \frac{\exp(-Z^2 4\ln 2/W_{\mathrm{D}}^2)}{(X-Z)^2 + (W_{\mathrm{L}}/2)^2}\,\mathrm{d}z, \quad (1)$$

where $\Phi(X)$ is the Voigt function whose frequency integral is normalised to unity; X is the frequency shift relative to the centre of the $^2P_{1/2}(F = 3) \rightarrow {}^2P_{3/2}(F = 4)$ transition line; ΔN is the inverse population density on this transition; A_{34} is the transition probability; $\lambda = 1.315$ μm is the wavelength.

The Gaussian component in the amplification line spectrum is caused by the Doppler broadening and has the width W_{D}. For iodine atoms, this width depends on the gas flow temperature as $W_{\mathrm{D}} = 14.49\sqrt{T}$, where T is the flow temperature in Kelvins and W_{D} is measured in megahertz. The Lorentzian component in the amplification line spectrum is caused by collision broadening resulting from the interaction of iodine atoms with the gas components. The collision width is proportional to the partial pressure of each gas component and is additive: $W_{\mathrm{L}} = \sum \alpha_i p_i f_i(300\,\mathrm{K}/T)$, where α_i is the collision broadening coefficient for the ith gas at a temperature of 300 K; p_i is the partial pressure of the ith gas; $f_i(1) = 1$.

Therefore, the coefficient α_i is the parameter of broadening at $T = 300$ K. The theory predicts that the function $f_i(300\,\mathrm{K}/T)$ increases with decreasing temperature. For example, if a perturbing particle separated from the atom by a distance R causes the shift of the transition frequency by $\Delta\nu = CR^{-6}$ (C is a constant), the theory predicts the temperature dependence $f(300\,\mathrm{K}/T) = (300\,\mathrm{K}/T)^{0.7}$. For the shift $\Delta\nu = CR^{-3}$, the temperature dependence has the form $f(300\,\mathrm{K}/T) = 300\ \mathrm{K}/T$ [8]. If the transition frequency shift has the same power dependence on R in the interaction of iodine atoms with any gas component, the collision width can be represented as

$$W_{\mathrm{L}} = f(300\,\mathrm{K}/T) \sum \alpha_i p_i. \quad (2)$$

Taking this into account, we determined the temperature dependence $f(300\,\mathrm{K}/T)$ in the temperature range 220 – 340 K which is typical of the active medium of an OIL. To prepare a low-temperature gas medium containing atomic iodine, we used the method of preparing a cold active medium of a subsonic OIL, in which iodine atoms are produced due to dissociation of molecular iodine in singlet oxygen [9].

M V Zagidullin, V D Nikolaev, M I Svistun, N A Khvatov P N Lebedev Physics Institute, Samara Branch, Russian Academy of Sciences, Novo-Sadovaya ul. 221, 443011 Samara, Russia

Received 6 December 2000
Kvantovaya Elektronika **31** (4) 373 – 376 (2001)
Translated by E N Ragozin

2. Experimental

As a medium containing atomic iodine, we used the active medium of an oxygen–iodine laser whose temperature could be lowered to 220 K. Fig. 1 shows the schematic of the setup. Singlet oxygen $O_2(^1\Delta)$ was produced in a jet generator of singlet oxygen (GSO) upon the interaction of the jets of alkaline solution of hydrogen peroxide and the chlorine flow. The design and the operation of the GSO, as well as the flow-through section of the oxygen–iodine laser, are described in Ref. [10]. The chlorine utilisation factor in the reactor was 95 %.

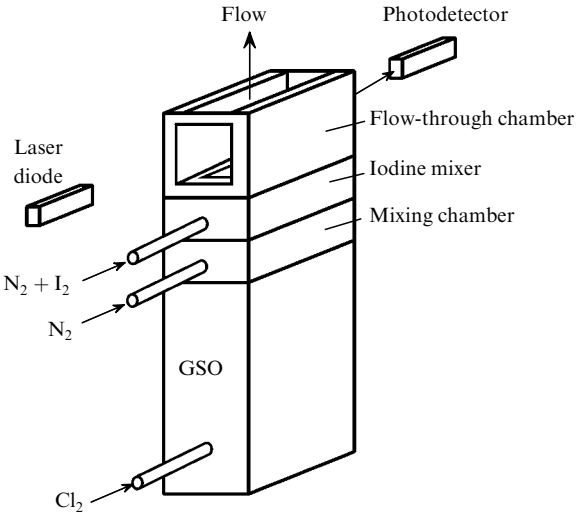

Figure 1. Schematic of the setup for producing the medium with atomic iodine and its diagnostics using a tunable semiconductor laser.

The temperature of the alkaline solution of hydrogen peroxide was −16°C in all runs. Primary nitrogen was admixed to the oxygen flow in the mixing chamber. Then, a mixture of secondary nitrogen with molecular iodine vapour was added to the $O_2(^1\Delta) + N_2$ flow via an iodine mixer. During the mixing of these flows, a partial dissociation of the molecular iodine to atoms occured, like in an OIL. The resultant gas mixture entered the flow-through chamber in which the atomic iodine amplification $^2P_{1/2}(F = 3) \rightarrow {}^2P_{3/2}$ $(F = 4)$ line was scanned by the beam of a tunable semiconductor laser.

The flow-through chamber cross section for the flow was 50 mm × 28 mm. The chamber side walls were optical wedges through which the semiconductor laser beam was introduced into the chamber. The gas flow temperature could be varied by changing: the temperature of primary nitrogen, the flow rate of the primary nitrogen, and the flow rate of molecular iodine.

To obtain low temperatures of the gas flow, the primary nitrogen was blown through a copper helix immersed in a vessel with liquid nitrogen. A variation in the flow rate of molecular iodine results in a variation in the quenching rate of the energy stored in $O_2(^1\Delta)$ and, hence, in a variation in the flow temperature. The gas mixture was evacuated using a pump with a capacity of 125 litre s^{-1}.

Under these conditions, the gas velocity in the flow-through chamber was essentially subsonic. Pressures were measured with 'Sapfir' pickups. The error of pressure measurements was of the order of 1 %. To ensure sufficient amplification in the spectral wings, where the main contribution to the broadening is made by the Lorentzian component, the experiments were performed for a gas flow pressure in the flow-through chamber above 10 Torr. Only in this case it was possible to reliably separate Lorentzian and Gaussian components in the amplification spectrum.

The atomic iodine amplification (absorption) spectrum at the strongest $^2P_{1/2}(F = 3) \rightarrow {}^2P_{3/2}$ $(F = 4)$ transition was scanned, using a high-resolution spectroscopy diode laser complex of Physical Science Inc. (USA) placed at our disposal by the US Air-Force Research Laboratory. The scanning laser radiation was directed to the flow-through chamber and was recorded with a photodetector. The hardware and the software of the complex allowed real-time measurements of the absorption spectrum. The scanning laser frequency was varied within the limits ±1500 MHz relative to the line centre of the $^2P_{1/2}(F = 3) \rightarrow {}^2P_{3/2}(F = 4)$ transition line. The initial diameter of the scanning laser beam was 3 mm. The spectral shape of the probe laser line was close to a Lorentzian with the width $W_{las} \approx 8$ MHz.

3. Results

Fig. 2 shows the spectrum of the amplification line under the conditions providing the positive inverse population on the $^2P_{1/2}(F = 3) \rightarrow {}^2P_{3/2}(F = 4)$ transition in the flow-through chamber. In some experiments, we studied the absorption lines that appears when $O_2(^1\Delta)$ was quenched due to the increase in the iodine flow rate and the temperature of the gas flow increased. The Lorentzian component of the Voigt function contains the width of the probe laser radiation $W_{las} \approx 8$ MHz, so that the true collision width was determined from the relation $W_L = W_{L1} - W_{las}$, where W_{L1} is the width of the Lorentzian component in the amplification spectrum. When the magnitudes of W_D and W_{L1} are comparable, the mathematical processing of the amplification spectrum allows one to separate reliably Lorentzian and Gaussian components in the amplification spectrum line and then to determine W_D, W_{L1}, and W_L.

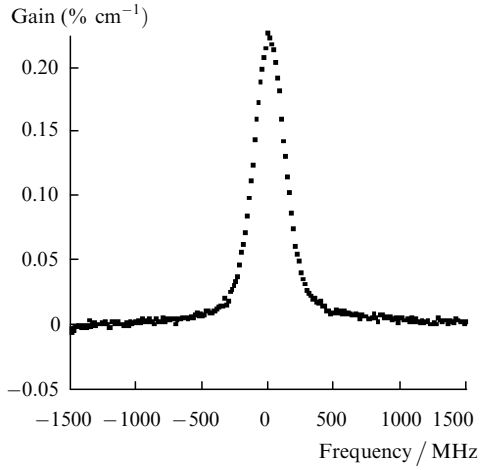

Figure 2. Spectrum of the amplification line at the $^2P_{1/2}(F = 3) \rightarrow {}^2P_{3/2}(F = 4)$ transition of atomic iodine.

Table 1 presents gas-dynamic experimental condition and the results obtained after mathematical processing of

Table 1. Gas-dynamic experimental conditions and results of processing the amplification spectrum.

M_{Cl_2}/ mmol s^{-1}	M_{NP}/ mmol s^{-1}	M_{NS}/ mmol s^{-1}	p_1 / Torr	p_2 / Torr	p_{N_2} / Torr	p_{O_2} / Torr	p_{Cl_2} / Torr	p_{H_2O} / Torr	W_D	W_{L1}	T/K
10	60.6	10	17.7	14.2	12.4	1.59	0.088	0.100	215	112	220
10	52.6	10	16.3	13.1	11.3	1.62	0.090	0.111	215	102	220
10	62.3	10	18.4	14.6	12.8	1.60	0.089	0.096	216	113	222
10	60.6	10	20.2	14	12.3	1.56	0.087	0.086	226	99	243
10	60.6	10	18.3	14	12.3	1.56	0.087	0.095	231	91	254
10	41.6	10	16.6	11.1	9.3	1.62	0.090	0.109	234	76	261
10	41.6	10	16.6	11	9.2	1.61	0.089	0.108	239	74	272
10	48	10	16.7	12	10.2	1.59	0.088	0.106	243	81	281
20	69.2	10	24.1	17	13.6	3.08	0.171	0.142	248	108	293
20	41.6	10	18.3	12.8	9.2	3.22	0.179	0.195	254	82	307
10	69.7	10	22.2	15.4	13.7	1.55	0.086	0.077	262	92	327
10	48	10	17.1	12	10.2	1.59	0.088	0.103	268	69	342
10	48	10	17.3	12	10.2	1.59	0.088	0.102	270	69	347

the amplification spectrum. The errors of measurement of W_D and W_{L1} were within 2 and 4 %, respectively. These errors appear because it is impossible to unambiguously separate the Lorentzian and Gaussian components in the presence of noise in the spectrum.

Table 1 also gives the component composition of the gas flow calculated in the following way. The total molar gas flow rate M through the flow-through chamber is primarily determined by the flow rates chlorine M_{Cl_2}, primary nitrogen M_{NP}, and secondary nitrogen M_{NS}: $M = M_{Cl_2} + M_{NP} + M_{NS}$. In addition, in the gas flow there exists water vapour, which comes with the oxygen from the GSO, and also atomic and molecular iodine.

Under our experimental conditions, the chlorine utilisation factor in the GSO was 95 %. Therefore, the partial oxygen pressure in the gas flow is $p_{O_2} = p_2 M_{Cl_2} U/M$ and the partial chlorine pressure is $p_{Cl_2} = p_2 M_{Cl_2}(1 - U)/M$ (p_2 is the pressure in the flow-through chamber). The water vapour pressure in the GSO is close to the saturation vapour pressure $p_s = 1.5$ Torr above the alkaline solution of hydrogen peroxide at $-16\,^\circ$C. The ratio of the water vapour concentration to that of the active gas (oxygen + chlorine) in the GSO and in the flow-through chamber should be equal if the condensation of water vapour or the ejection of finely dispersed aerosol from the GSO do not occur. This allows us to estimate the partial pressure of water vapour in the gas mixture as $p_{H_2O} \approx (p_s/p_1)(M_{Cl_2}/M)p_2$ (p_1 is the pressure in the GSO). Upon mixing the oxygen with the precooled nitrogen, the actual partial pressure of water vapour is lower owing to its partial condensation.

The partial pressures of atomic and molecular iodine are most complicated to estimate separately, because the dissociation efficiency is unknown. However, because the flow rate of molecular iodine did not exceed 0.3 mmol s^{-1}, the relative contribution of the iodine component to the total collision width was within 1 % and was neglected.

Table 2. Collision broadening coefficients for the $^2P_{1/2} \rightarrow {}^2P_{3/2}$ transition in atomic iodine for the above medium components at $T = 300$ K.

Gas	α_i/MHz $Torr^{-1}$	References
O_2	5	[7]
N_2	5.5	[7]
Cl_2	6.3	[11]
H_2O	20.6	[11]
I_2	10.5	[4]
I	4.4	[4]

In the analysis of the temperature dependence of collision broadening, the temperature dependences of the collision broadening coefficients were assumed to be identical for all components of the active gas medium. In this case, the collision line width is determined by formula (2). Table 2 presents the collision broadening coefficients for the above medium components at 300 K.

Therefore, neglecting the contribution of the iodine component to the collision broadening, the collision width measured in megahertz can be approximated as

$$W_L = (5p_{O_2} + 5.5p_{N_2} + 6.2p_{Cl_2} + 20.6p_{H_2O}) f(300\,\mathrm{K}/T). \quad (3)$$

Assuming that $f(300\,\mathrm{K}/T) = (300\,\mathrm{K}/T)^\gamma$ and using the relation $W_L = W_{L1} - 8$, Eqn (3) can be written as

$$f\left(\frac{300\,\mathrm{K}}{T}\right) = \left(\frac{300\,\mathrm{K}}{T}\right)^\gamma = \frac{W_{L1} - 8}{5p_{O_2} + 5.5p_{N_2} + 6.2p_{Cl_2} + 20.6p_{H_2O}}. \quad (4)$$

Fig. 3 shows the dependence $f(300\,\mathrm{K}/T)$ for parameters given in Table 1. Also are shown the errors of measuring $f(300\,\mathrm{K}/T)$ and T, which are determined by the measurement errors for W_{L1}, W_D, and p_2. The best fit of the experimental data by the function $(300\,\mathrm{K}/T)^\gamma$ by the method of least squares was achieved at $\gamma = 0.82$. However, our analysis showed that the function $(300\,\mathrm{K}/T)^\gamma$ ($0.75 < \gamma < 1$) in the 220–347 K temperature range lies within the measurement error interval, and the possible values are $\gamma = 0.87 \pm 0.13$.

4. Conclusions

According to the collision broadening theory, the collision width depends on the temperature as $(300\,\mathrm{K}/T)^\gamma$. Our experimental data are satisfactorily described by the temperature dependence of the collision width $W_L \sim (300\,\mathrm{K}/T)^\gamma$, where $\gamma = 0.87 \pm 0.13$. To refine the values of γ, the col-

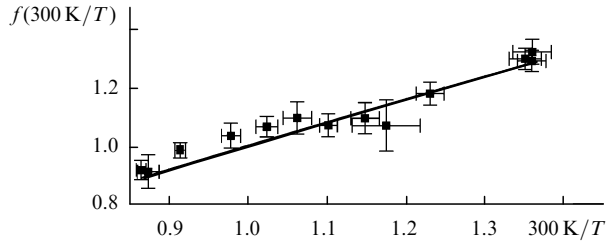

Figure 3. Experimental function $f(300\,\mathrm{K}/T)$ (points) and function $(300\,\mathrm{K}/T)^{0.82}$ (line).

lision width should be measured at temperatures well below 200 K, because the function $(300\,\mathrm{K}/T)^{\gamma}$ in this case depends more strongly on γ.

The results obtained may prove to be highly useful in the remote contact-free measurements of the static pressure in supersonic flows of the active medium of an oxygen – iodine laser.

Acknowledgements. The authors thank the US Air-Force Research Laboratory for placing at our disposal the diagnostic complex (based on high-resolution diode laser spectroscopy) of Physical Science Inc. (USA), B T Anderson and R F Tate for their assistance at the initial stage of the work with this complex, and G D Hager for discussing the results of this work. This work was supported by the European Office for Aerospace Research and Development (USA) under an ISTC Contract No. 1862-P.

References

1. Zuev V S, Katulin V A, Nosach V Yu, Nosach O Yu *Zh. Eksp. Teor. Fiz.* **62** 1673 (1972)
2. Patrick T D, Palmer R E *J. Chem. Phys.* **62** 3350 (1975)
3. Neuman D K, Clarck P K, Shea R F, Davis S J *J. Chem. Phys.* **79** 4680 (1983)
4. Engelman R, Palmer B, Davis S J *J. Opt. Soc. Am.* **73** 1585 (1983)
5. Cerny D, Aubert-Frecon M, Basic R, Bussery B, Nota M, Verges J *Proc. SPIE Int. Soc. Opt. Eng.* **1031** 312 (1988)
6. Tate R F, Hunt B S, Helms C A, Truesdell K A, Hager G D *IEEE J. Quantum Electron.* **31** 1632 (1995)
7. Davis S J, Kessler W J, Bachmann M *Proc. SPIE Int. Soc. Opt. Eng.* **3612** 157 (1999)
8. Sobelman I I, Vainshtein L A, Yukov E A *Excitation of Atoms and Broadening of Spectral Lines* (Berlin: Springer-Verlag, 1981)
9. Zagidullin M V, Nikolaev V D, Svistun M I, Khvatov N A *Kvantovaya Elektron.* **25** 413 (1998) [*Quantum Electron.* **28** 400 (1998)]
10. Zagidullin M V, Nikolaev V D, Svistun M I, Khvatov N A *Kvantovaya Elektron.* **30** 161 (2000) [*Quantum Electron.* **30** 161 (2000)]
11. Carroll D L *AIAA J.* **33** 1454 (1995)